ACS Medicinal Chemistry Letters

pubs.acs.org/acsmedchemlett

Letter

Apoptosis Inducing 1,3,4-Oxadiazole Conjugates of Capsaicin: Their *In Vitro* Antiproliferative and *In Silico* Studies

Fatima Naaz, Faiz Ahmad, Bilal Ahmad Lone, Arif Khan, Kalicharan Sharma, IntzarAli, M. ShaharYar, Yuba Raj Pokharel,* and Syed Shafi*

Cite This: *ACS Med. Chem. Lett.* 2021, 12, 1694−1702

Read Online

ACCESS | Metrics & More | Article Recommendations | Supporting Information

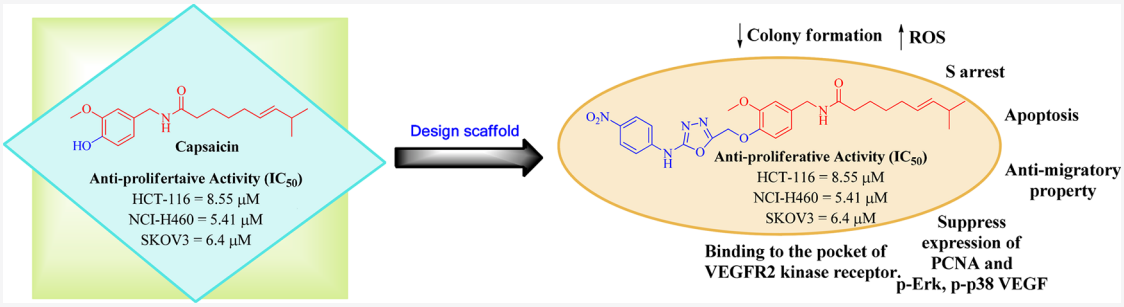

ABSTRACT: A series of 1,3,4-oxadiazole tethered capsaicin derivatives was prepared by using one point modification at the vanillyl-hydroxyl group of capsaicin. All the prepared capsaicinoids were evaluated for their antiproliferative activity against NCI-60 human cancer cell lines at 10 μM. Among the compounds tested, compound **20a** exhibited good cytotoxic activity against HCT-116, NCI-H460, and SKOV3 cell lines with IC_{50} 8.55 μM, 5.41 μM, and 6.4 μM, respectively, compared to the parent natural product capsaicin. Further on, it significantly inhibited the colony formation in NCI-H460 in a dose dependent manner and enhanced the ROS effect. It also caused cell arrest at the S phase and induced apoptosis via suppressing the Pro parp marker. Compound **20a** exhibited an antimigratory property and suppressed the expression of the VEGF marker in a dose dependent manner. Furthermore, compound **20a** also suppressed the effects of the p-Erk, p-p38, and P-CNA makers. *In silico* studies supported the interaction of this class of compounds with the VEGFR2 protein.

KEYWORDS: *Capsaicin, cancer, antiproliferative, 1,3,4-oxadiazole, VEGFR*

Worldwide capsaicin (**1**) is known for its pungent flavor and is consumed in a variety of foods as an additive. Basically, it is an amide derivative of vanillyl amine and C-10 fatty acid. It has been isolated from *capsicum annum* and *capsicum frutescence* of genus Capsicum, family Solanaceae. Apart from capsaicin, various other pungent metabolites known as capsaicinoids (**2**−**10**) are also found from the pepper plant (Figure 1). Among all the capsaicinoids, capsaicin (**1**) and dihydrocapsaicin (**2**) exist in abundances of 80−90% in peppers.[1] Medicinally, capsaicin is used as an analgesic agent in the form of several topical formulations/creams/patches that are used to relieve pain.[2]

Capsaicin has demonstrated a broad spectrum of biological activities including antiproliferative activity,[3−14] anti-inflammatory activity, antilipase activity (anti obesity), NorA efflux pump inhibition,[15] HDAC inhibition,[16] controlling glucose metabolism,[17] etc. Capsaicin was also found to enhance the digestion of foods by increasing the enzymatic activity of the gut.[18] Capsaicin was found to be a robust apoptotic inducer in several forms of human cancer cells both in mice models and *in vitro*.[19] From the literature, several studies explained the viable anticancer drug applicability of capsaicin for curing human small cell lung cancer, breast cancer, prostate cancer, and colon cancers. Inspired by its anticancer properties, its mechanism of action has been intensively studied and various mechanisms for the anticancer property of capsaicin have been proposed.[15] One of the broadly believed mechanisms is interaction of capsaicin with transient receptor potential vanilloids (TRPVs). TRPVs stimulate the Ca^{2+}-mediated mitochondrial damage that leads to the release of *cytochrome-C* which ultimately causes the cell apoptosis (Figure 2).[15,16]

Apart from its beneficial properties, capsaicin demonstrated some of the side effect. At high doses capsaicin induced stomach ulcers and accelerated the expansion of various cancer types such as stomach, prostate, liver, duodenal, etc. and was also found to increase breast cancer metastasis.[17]

Received: May 27, 2021
Accepted: October 18, 2021
Published: October 21, 2021

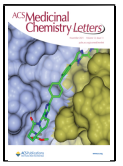

https://doi.org/10.1021/acsmedchemlett.1c00304
ACS Med. Chem. Lett. 2021, 12, 1694−1702

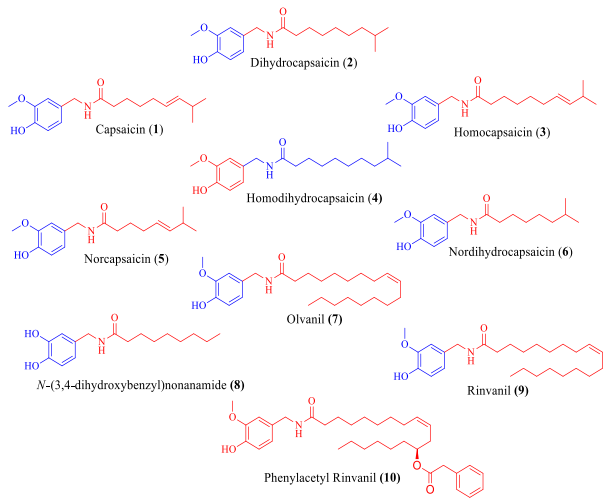

Figure 1. Chemical structures of different capsaicinoids.

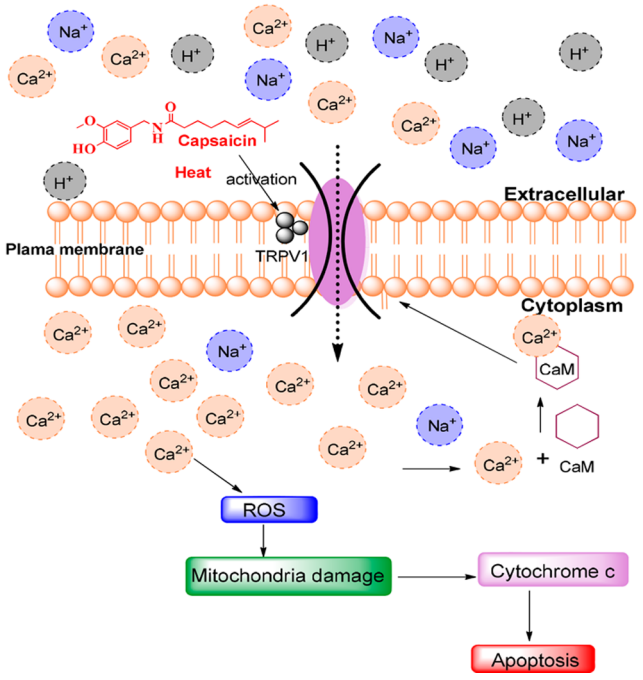

Figure 2. Reported mechanism of action of capsaicin.

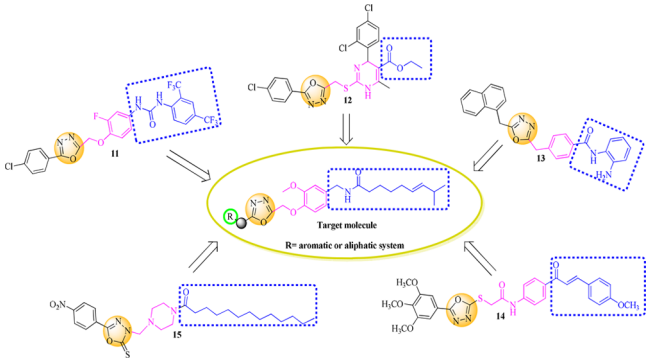

Figure 3. Rational approach to designed semisynthetic capsaicin analogues.

Furthermore, it cannot be handled freely as it has a strong pungent flavor which causes a burning sensation to the skin.[18]

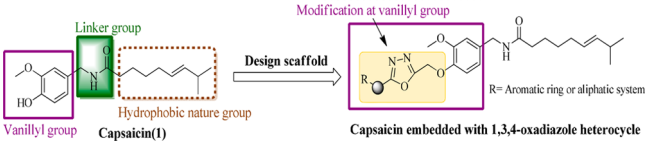

Figure 4. Design scaffold of target compounds from capsaicin.

Scheme 1. Systematic Scheme for Preparation of Target Conjugated 20a–k[a]

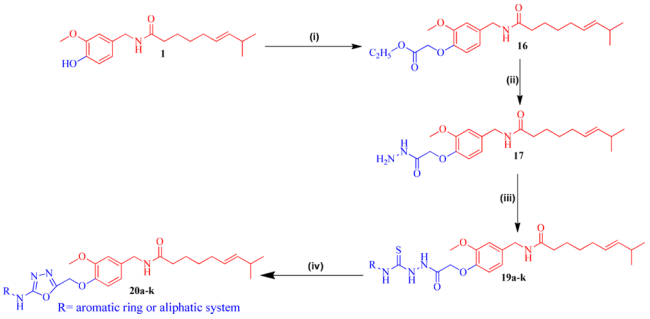

[a]Reagents and condition: (i) $CH_3COOCH_2CH_2Br$, K_2CO_3, acetone, reflux at K_2CO_3, acetone reflux at 60–70 °C for 48 h. Yield: 99%. (ii) $NH_2NH_2{\cdot}H_2O$, RT for 8 h. Yield: 98%. (iii) RNCS (**18a–k**), EtOH, reflux for 6 h at 60–70 °C. Yield: 95%. (iv) EDC·HCl, cat. HOBt, dry DMF, RT for 3–5 h. Yield: 78–98%.

Scheme 2. Systematic Scheme for Preparation of Target Conjugated 22a and 22b[a]

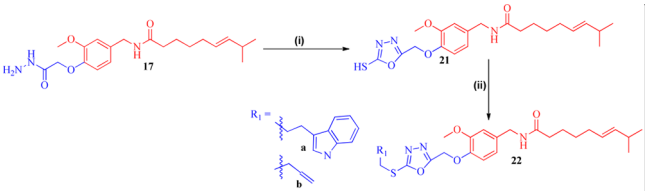

[a]Reagents and conditions: (i) CS_2, KOH, EtOH, refluxed at 70 °C. Yield: 83%. (ii) $R1CH_2Br$, dry DMF, TEA, RT. Yield: 86–89%.

Capsaicin, when exposed to the naked eye, causes conjunctivitis, intense tearing, pain, and blepharospasm.[19] Moreover capsaicin illustrated an antiproliferative profile with a range from 5 μM to 400 μM against various human cancer cell lines.[20]

On the other hand, 1,3,4-oxadiazole moieties have emerged a privileged gibbet in cancer drug discovery. Various 1,3,4-oxadiazole containing compounds (**11–15**) have demonstrated a broad spectrum of antiproliferative activity against different cancer cell lines[21,22] (see Figure 3). Herein, compound **11** illustrated antiproliferative activity in the submicromolar range with IC_{50} values of 0.67 μM, 0.80 μM, and 0.87 μM against PC-3, HCT-116, and ACHN, respectively.[21] Compounds **12** and **13**, bearing 1,3,4-oxadiazole moieties, also demonstrated good cytotoxicity, whereas compound **13** demonstrated cytotoxicity in nanomolar concentration with IC_{50} 80 nM against the MOLT-4 cancer cell line.[23,24] Further on, compound **14** displayed a promising cytotoxic activity against several cancer cell lines, with IC_{50} values ranging between 1.95 and 3.45 μM.[25] Compound **15** exhibited good activities against 4T1 memory cancer cells and CT26 WT colon cancer cells with IC_{50} 5.2 μM and 11.7 μM, respectively.[22]

https://doi.org/10.1021/acsmedchemlett.1c00304
ACS Med. Chem. Lett. 2021, 12, 1694–1702

Table 1. Structure of All the Synthesized 1,3,4-Oxadizole Conjugates of Capsaicin (20a−k) with Their Respective Thiosemicarbazides (19a−k)

Code	Thiosemicarbazide (19a-k)	Capsaicin linked 1,3,4-oxadizole moiety (20a-k)
a	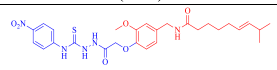	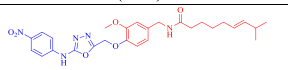
b	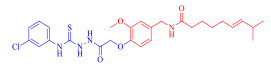	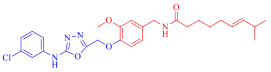
c	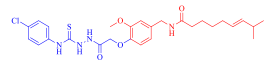	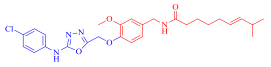
d	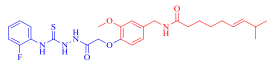	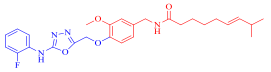
e	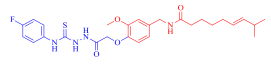	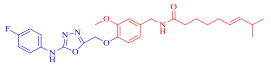
f	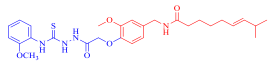	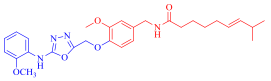
g	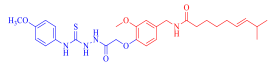	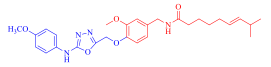
h	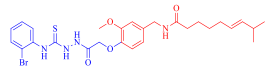	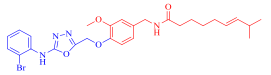
i	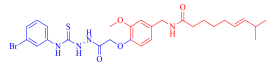	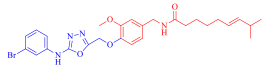
j	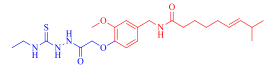	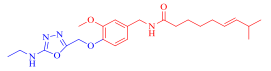

Table 2. Structures of All the Synthesized 1,3,4-Oxadizole Conjugates of Capsaicin

21	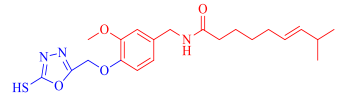
22a	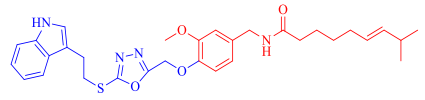
22b	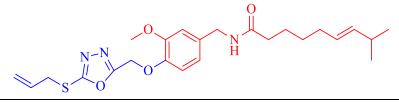

Keeping in view the low anticancer activity profile of capsaicin with its above-mentioned side effects[17] and the significance of the 1,3,4-oxadiazole moiety in the vicinity of the cancer, we aim to design some new capsaicin based secondary leads with improved antiproliferative activity. In this regard, modifications at the vanillyl hydroxyl group of capsaicin have been envisaged and a small library of 1,3,4-oxadiazole conjugates have developed as shown in Figure 4.

The designed compounds **20a−k**, **21**, and **22a−b** were prepared via the multistep strategy shown in Schemes 1 and 2. α-Bromoethyl acetate was reacted with capsaicin (**1**) to afford capsaicin ester (**16**). This ester was further treated with hydrazine hydrate to yield hydrazide (**17**). Herein, hydrazide (**17**) was further treated with various aromatic/aliphatic isothiocyanides (**18a−k**) under refluxing conditions in absolute alcohol to afford the corresponding thiosemicarbazides (**19a−k**). EDC catalyzed cyclization of thiosemicarbazides (**19a−k**) finally afforded the target compounds (**20a−k**) in 83−95% yield as illustrated in Scheme 1 and Table 1.

In addition, intermediate hydrazide (**17**) was reacted with carbon disulfide (CS_2) in the presence of potassium hydroxide to yield 5-mercapto-(1,3,4-oxadiazole) bound capsaicin conjugate **21**. Intermediate **21**, upon reacting with 3-(2-bromoethyl)indole and allyl bromide, has formed corresponding conjugates **22a** and **22b** in the presence of triethylamine with high yields (86−93%) as demonstrated in Scheme 2 and Table 2.

Formation of ester derivative **16** was definite by the presence of a singlet corresponding to two protons at δ 4.71 ppm (-OCH_2-), characteristic signals for the ethyl ester (-$COOCH_2CH_3$), and the absence of the phenolic -OH group of capcaisin at δ 8.83 ppm.

The appearance of a broad singlet at δ 4.33 ppm corresponds to an -NH_2 group, a triplet at δ 8.25−8.22 ppm corresponds to the -NH- of -CONH-NH_2, and the absence of the peaks corresponds to the ethyl goup of the ester, confirming the formation of hydrazide **17** from ester **16**. Conversion of thiosemicarbazides (**19a−k**) from hydrazide (**17**) was recognized by the presence of four singlets corresponding to -NH- groups at δ 11.66 ppm, 10.24 ppm, 10.09 ppm, and 9.99 ppm and the presence of additional aromatic protons in the range δ 8.24−7.88 ppm. Finally, formation of 1,3,4-oxadiazoles (**20a−k**) from respective thiosemcarbazides (**19a−k**) was affirmed by the presence of a singlet at δ 10.97 ppm (DMSO-d_6, ^{1}H NMR) or δ 8.26−7.05 ppm ($CDCl_3$, ^{1}H NMR) corresponding to the -NH- proton of the 2-amino-1,3,4-oxadiazole moiety, and the absence of signals corresponds to a thiosemicarbazide functionality. Further on, these -NH- groups are confirmed by D_2O proton exchange experiments.

Conversion of capsaicin hydrazide **17** to 5-mercapto-1,3,4-oxadiazole conjugate **21** was avowed by the presence of a singlet corresponding to the -SH group at δ 9.51 ppm. Formation of the target molecule **22a** was confirmed by the presence of two triplets corresponding to the ethylene (-CH_2-CH_2-) linker and the signals corresponding to the indole moiety. Finally, formation of the compounds was confirmed by HRMS and ESI-MS.

All the newly prepared compounds were proffered to the National Cancer Institute (Developmental Therapeutic Program), Bethesda, USA (www.dtp.nci.nih.gov). All the compounds were evaluated for their *in vitro* antiproliferative activity at 10 μM (single dose) against 60 cancer cell lines of the NCI panel under nine different cancer cell types with their subpanels as depicted in Table S1 of the Supporting Information. The screening result for all active compounds is reported as a growth percentage in Table 3.

Antiproliferative data revealed that compounds **20a** and **20d** exhibited cytotoxicity against various cancer cell lines as both compounds **20a** and **20d** exhibited excellent activity against OVCAR-4 and 786-0 with a range of percentage growth of 0.69−22.2. Compound **20a** showed an excellent activity against HOP-62, NCI-H460, HCT-116, OVCAR-8, SK-OV-3, and CAKI-1 with a % growth range of 0−33.6. Moreover, compound **20a** also displayed moderate cytotoxicity against the nonsmall cell lung cancer A549 cell line, CNS cancer SNB-19 cell line, CNS cancer U251 cell line, melanoma cancer SK-MEL-5 and UACC-62 cell line, renal cancer ACHN and

https://doi.org/10.1021/acsmedchemlett.1c00304
ACS Med. Chem. Lett. 2021, 12, 1694−1702

Table 3. Growth Percentage against 60 Human Cancer Cell Lines of the NCI Panel at 10 μM of the Active Conjugates[a]

Sub panel cancer cell line		Growth percentage			
		20a	20d	20i	22a
Leukemia	CCRF-CEM	78.85	82.95	81.76	**34.67**
	HL-60(TB)	101.03	89.70	79.77	**50.23**
	K-562	59.62	60.36	65.02	**40.71**
	MOLT-4	84.22	82.05	83.54	**29.16**
	RPMI-8226	52.34	64.91	70.31	nt
	SR	64.20	67.28	67.67	**49.30**
Nonsmall cell lung cancer	A549/ATCC	**49.02**	105.30	95.38	79.42
	EKVX	74.70	77.14	78.09	57.36
	HOP-62	**0**	56.40	75.58	92.77
	NCI-H226	62.14	64.53	**50.41**	67.25
	NCI-H23	62.14	63.80	66.01	66.57
	NCI-H322M	54.87	86.07	98.04	88.69
	NCI-H460	**33.48**	80.34	97.55	89.80
	NCI-H522	72.97	60.29	68.60	59.35
Colon cancer	COLO 205	70.91	104.24	109.93	71.22
	HCC-2998	83.57	90.82	100.83	97.97
	HCT-116	**24.55**	53.45	67.59	69.99
	HCT-15	81.17	90.10	90.22	68.56
	HT29	71.71	89.95	97.66	69.68
	KM12	71.65	78.80	90.31	73.28
	SW-620	67.32	98.94	95.44	84.70
CNS cancer	SF-268	79.65	**45.48**	92.63	78.89
	SF-295	64.90	**48.03**	84.25	68.78
	SF-539	70.24	**48.16**	88.44	80.83
	SNB-19	54.05	58.55	99.55	77.05
	SNB-75	**48.71**	57.78	83.48	83.14
	U251	**48.58**	83.96	101.81	80.52
Melanoma	LOX IMVI	55.24	83.41	88.92	55.24
	M14	69.64	99.73	93.30	nt
	MDA-MB-435	66.39	100.01	101.19	90.22
	SK-MEL-2	71.89	111.03	104.61	86.68
	SK-MEL-28	78.87	85.18	107.28	104.42
	SK-MEL-5	**46.26**	86.57	89.84	105.37
	UACC-257	77.56	98.18	105.03	100.67
	UACC-62	**39.61**	65.48	67.54	67.51
Ovarian cancer	IGROV1	53.49	58.44	92.89	73.71
	OVCAR-3	77.31	68.29	87.99	88.32
	OVCAR-4	**11.25**	**0.69**	85.10	71.67
	OVCAR-5	100.97	77.67	91.08	101.99
	OVCAR-8	**24.96**	**45.17**	98.03	71.26
	NCI/ADR-RES	79.62	**43.35**	87.04	56.51
	SK-OV-3	**11.82**	**48.61**	82.58	85.74
Renal cancer	786-0	**22.25**	**11.98**	95.60	89.26
	A498	56.81	92.53	77.79	73.28
	ACHN	**41.17**	56.05	85.14	76.55
	CAKI-1	**33.60**	nt	nt	nt
	RXF 393	54.11	68.76	70.61	54.00
	SN 12C	**49.04**	70.47	95.72	83.06
	TK-10	84.10	97.67	104.24	91.69
	UO-31	58.74	52.79	64.01	**45.03**
Prostate cancer	PC-3	**37.64**	72.50	87.90	56.85
	DU-145	62.03	88.70	89.79	94.93
Breast cancer	MCF7	55.23	66.88	83.70	58.79
	MDA-MB-231/ATCC	67.10	63.87	78.30	70.64
	HS 578T	63.17	83.68	93.67	81.05
	BT-549	108.01	76.95	76.43	75.03
	T-47D	**48.58**	65.02	58.86	**42.98**
	MDA-MB-468	53.75	58.92	48.07	**51.81**
	Mean GP	59.69	71.72	85.48	**72.88**

[a]nt = not tested; GP = growth percentage.

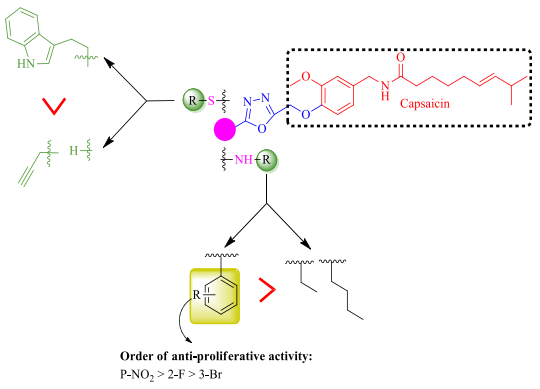

Figure 5. SAR for synthesized compounds against antiproliferative activity.

SN12C cell line, prostate PC-3 cancer cell line, and breast T-47D cancer cell line with growth % range of 37.6−49 while compound **20d** exhibited moderate activity against CNS cancer SF-268, SF-295, and SF-539 and ovarian cancer OVCAR-8, ADR-RES, and SK-OV-3 cell lines with a growth % range of 43.3−48.6. Among all other synthesized compounds, only compound **20i** demonstrated moderate activity against the NCI-H226 nonsmall lung cancer cell line with a growth percentage of 50.4.

Table 4. IC_{50} Profile for Compounds 20a, 20d, and 22a, with Capsaicin and Doxorubicin

Tested compound	IC_{50}		
	HCT-116	NCI-H460	SKOV3
20a	8.55 (μM)	5.41 (μM)	6.4 (μM)
20d	10.50 (μM)	14.42 (μM)	12.51 (μM)
22a	13.4 (μM)	9.89 (μM)	31.4 (μM)
Capsaicin	40.16 (μM)	30.66 (μM)	22.03 (μM)
Doxorubicin	57.77 (nM)	4.29 (nM)	25.83 (nM)

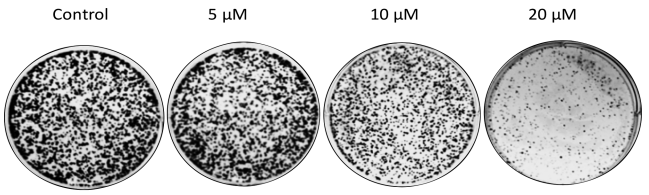

Figure 6. Treatment of compound **20a** suppressed the colony formation ability of NCI-H460. The clonogenicity of NCI-H460 was determined by a colony formation assay after the treatment of compound **20a**.

By considering other series of semisynthetic analogues of capsaicin, among all three synthesized compounds, compound

https://doi.org/10.1021/acsmedchemlett.1c00304
ACS Med. Chem. Lett. 2021, 12, 1694−1702

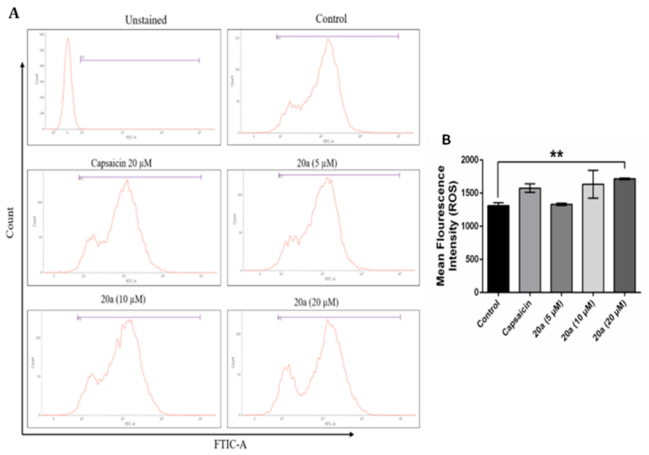

Figure 7. Compound **20a** treatment generates ROS in NCI-H460 cells. (A) Flow cytometric analysis demonstrated the levels of ROS in NCI-H460 treated with compound **20a**. (B) Bar representation for mean fluorescence intensity of compound **20a** in a NCI-H460 cell.

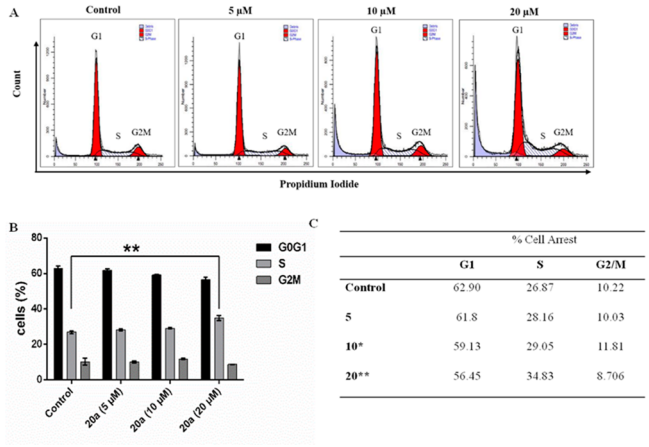

Figure 8. Compound **20a** promotes the S-phase cell cycle arrest in NCI-H460 cells. (A) Histogram of a representative experiment. (B) Data represented of mean ± SD of three independent experiments, where (**) indicates $P < 0.01$ compared to the vehicle control as determined by t test. (C) Table showing percentage cells in different phases of the cell cycle following the treatment with **20a** as compared to control.

22a (capsaicin tethered with indole moiety) showed susceptibility against all the cancer cell lines of leukemia with excellent activity against the CCRF-CEM and MOLT-4 leukemia cancer cell lines with % growths of 34.6 and 29.1. It also displayed good cytotoxicity against renal UO-31, breast T-47D, and breast MDA-MB-468 cancer cell lines with percentage growths of 40−51.8.

On the basis of the obtained NCI-antiproliferative results, SAR of the synthesized compounds was developed on two parameters: (i) types of the substitution attached to -NH/-S; (ii) types of the substituents on the aromatic ring (Figure 5).

Compounds with aromatic substitution (**20a, 20d, 20i, 22a**) to -NH/-S- demonstrated antiproliferative activity, while compounds with aliphatic substitution (**20j, 20k, 21, 22b**) resulted in loss of activity. So, the preference for antiproliferative activity to the group attach to -NH/-S is aromatic > aliphatic.

On the basis of the functional group attached to the aromatic ring, it has been seen that the analogues with electron

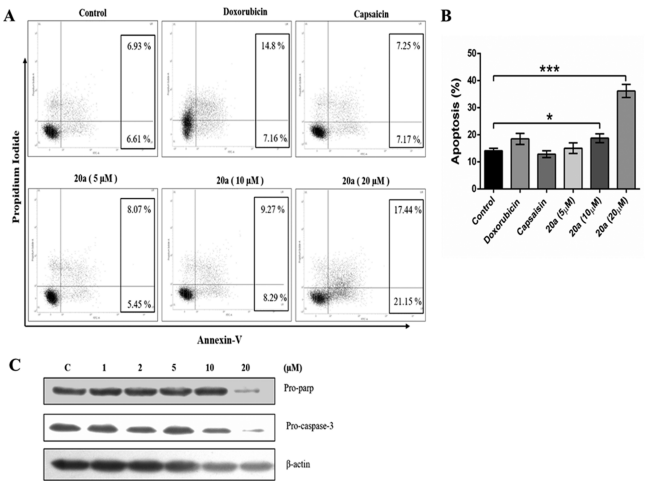

Figure 9. Compound **20a** induced apoptosis in NCI-H460 cells. (A) Flow cytometric analysis demonstrated the levels of apoptosis in NCI-H460. (B) Quantitative analysis of apoptosis. Data represents the mean ± SD of the percentage of apoptotic cells ($n = 3$), *$p < 0.05$, ***$p < 0.001$, compared to the vehicle control as determined by t test. (C) Western blot analysis of the effect of compound **20a** on the levels of Pro-parp and Pro-caspase 3 proteins in NCI-H460.

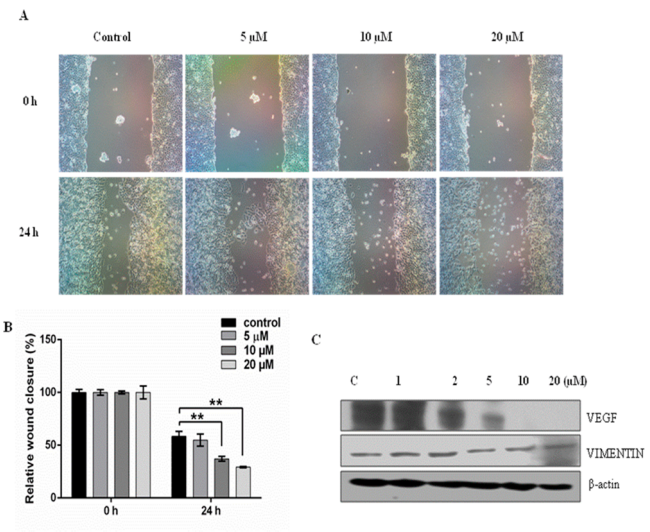

Figure 10. Compound **20a** inhibited the migration capacities of NCI-H460 cells. (A) Representative images of the wound healing assay carried out on NCI-H460 cells treated at 5 μM, 10 μM, and 20 μM. A significant open wound area was observed after the 24 h time point in both 10 and 20 μM treated NCI-H460 cells. The wound area was quantified by ImageJsoftware. Data is the representation of three independent experiments ± S. D. **$p < 0.01$, ***$p < 0.001$. (B) Graph representing a dose dependent antimigration effect of **20a** in a time interval of 24 h. (C) Effect of compound **20a** on the expression of Vimentin and VEGF. A suppression effect on the expression of VEGF was observed in a dose dependent manner (at 1 μM, 2 μM, 5 μM, 10 μM, and 20 μM), while no change in the expression of vimentin marker was observed.

withdrawing groups (**20a, 20d, 20i**) displayed more antiproliferative activity than the electron donating group and the order of the activity for the electron withdrawing group is NO_2 > F > Br.

Potent compounds **20a, 20d**, and **22a** obtained from the preliminary screening (NCI-antiproliferative data) were further evaluated for their IC_{50} values against HCT-116, NCI-H60,

https://doi.org/10.1021/acsmedchemlett.1c00304
ACS Med. Chem. Lett. 2021, 12, 1694−1702

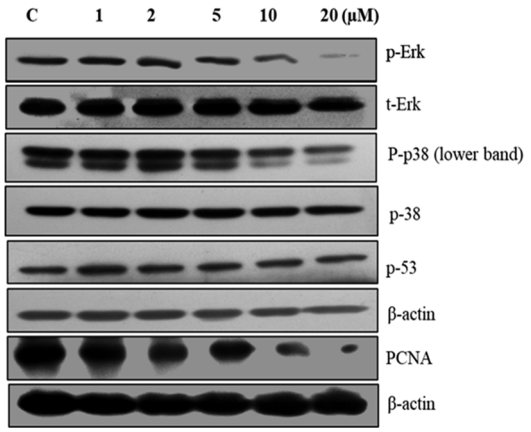

Figure 11. Effect of compound **20a** on major proteins related to cell proliferation. Expression levels of PCNA, p-53, p-38, P-p38, t-Erk, and p-Erk proteins determined by Western blot analysis in a dose dependent manner.

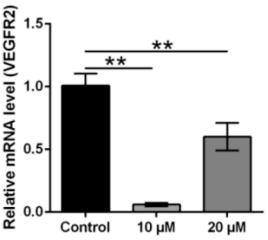

Figure 12. 20a treatment suppressed the VEGFR2 mRNA expression level: Quantification of VEGF gene expression in control and **20a** treated cells using real-time qPCR. GAPDH was used as internal control. The mean ± is shown in bar plots ($n = 3$). $^{**}p < 0.01$, $^{***}p < 0.001$.

Table 5. Docking Score of All Compounds in the Catalytic Binding Pocket of VEGFR2 Kinase Receptor (PDBID: 2QU5)

S. no	Code	Docking score (kcal/mol)
1	**20a**	−7.996
2	**20b**	−7.733
3	**20c**	−8.683
4	**20d**	−10.016
5	**20e**	−7.987
6	**20f**	−8.666
7	**20g**	−8.364
8	**20h**	−7.813
9	**20i**	−8.832
10	**20j**	−7.486
11	**20k**	−6.865
12	**2l**	−7.229
13	**22a**	−7.528
14	**22b**	−8.072
15	**Capaiscin**	−7.866
16	**Sunitinib**	−9.799

and SKOV3 by crystal violet assay. Doxorubicin was used as standard, and capsaicin was used as reference compound. Among these three compounds, compound **20a** has demonstrated potential antiproliferative activity with IC_{50s} 8.55 μM, 5.41 μM, and 6.4 μM against HCT-116, NCI-H460, and SKOV3, respectively. Herein compound **20d** exhibited moderate antiproliferative activity with IC_{50s} 10.50 μM, 14.42 μM, and 12.51 μM against HCT-116, NCI-H460, and SKOV3, respectively. Further on, compound **22a** demonstrated IC_{50}13.4 μM, 9.89 μM, and 31.4 μM against HCT-116, NCI-H460, and SKOV3, respectively (Table 4). Capsaicin exhibited antiproliferative activity against HCT-116, NCI-H460, and SKOV3 with IC_{50} of 40.16 μM, 30.66 μM, and 22.03 μM, respectively. While doxorubicin (standard) was demonstrated to have cytotoxic activity against HCT-116, NCI-H460, and SKOV3 cell lines with IC_{50s} of 57.77 nM, 4.29 nM, and 25.83 nM, respectively.

All three tested compounds exhibited better antiproliferative activity in comparison to capsaicin, but compound **20a** illustrated good cytotoxicity against NCI-H460 with IC_{50} of 5.41 μM among all. Compound **20a** was further evaluated for its toxicity against normal PNT2 cells (normal prostatic epithelial cells). Compound **20a** did not induced toxicity against the normal cell line even at 4-fold higher concentration of the IC_{50} value (Supporting Information). The most promising compound **20a** was further preceded with the mechanistic studies.

To explore whether the compound **20a** treatment affects the oncogenic behavior of lung cancer cells (NCI-H460), the colony formation assay was performed. Results demonstrated that treatment of compound **20a** decreases the colony formation of NCI-H40 cells in a dose dependent manner (at 5 μM, 10 μM, and 20 μM) compared with control as illustrated in Figure 6.

To examine the effect of compound **20a** on reactive oxygen species (ROS) formation in NCI-H460 cancer cells, these cells were treated with compound **20a** in a dose dependent manner (5 μM, 10 μM, and 20 μM) and it was observed that the treatment led to intracellular ROS generation as detected by H2DCFDA staining using a flow cytometer. As shown in Figure 7, the treatment of compound **20a** significantly increased the ROS production at 20 μM concentration compared to control.

To determine whether the treatment of compound **20a** influenced the cell cycle of NCI-H460, the cells were treated with compound **20a** in a dose dependent manner. These cells were stained with propidium iodide and evaluated using a flow cytometer. As shown in Figure 8(A, B), compound **20a** significantly lead to an increase of cells in the S phase of the cell cycle from 26.87 to 34.83 at 20 μM concentration. The cell percentages in different phases of the cell cycle are illustrated in Figure 8(C).

Annexin V/propidium iodide staining was performed to investigate the effect of compound **20a** on cell apoptosis. As depicted in Figure 9, the apoptotic index of NCI-H460 was significantly increased in compound **20a** treated cells at 20 μM concentration compared to control, doxorubicin, and capsaicin treated cells which promoted the apoptosis in lung cancer NCI-H460 cells.

Further on, the effect of compound **20a** treatment on the expression of proteins that regulate apoptosis was investigated. Western blotting analysis demonstrated that treatment of compound **20a** effectively decreased the expression levels of pro-parp and pro-caspase 3 molecules, indicating that treatment of compound **20a** promotes apoptosis.

A wound healing assay was done to check the antimigrating effect of compound **20a** on NCI-H460 cancer cells. As shown in Figure 10, the artificial wound gap of control cells significantly decreased compared with compound **20a** treated cells as observed after a gap of 24 h. It was observed that the

https://doi.org/10.1021/acsmedchemlett.1c00304
ACS Med. Chem. Lett. 2021, 12, 1694−1702

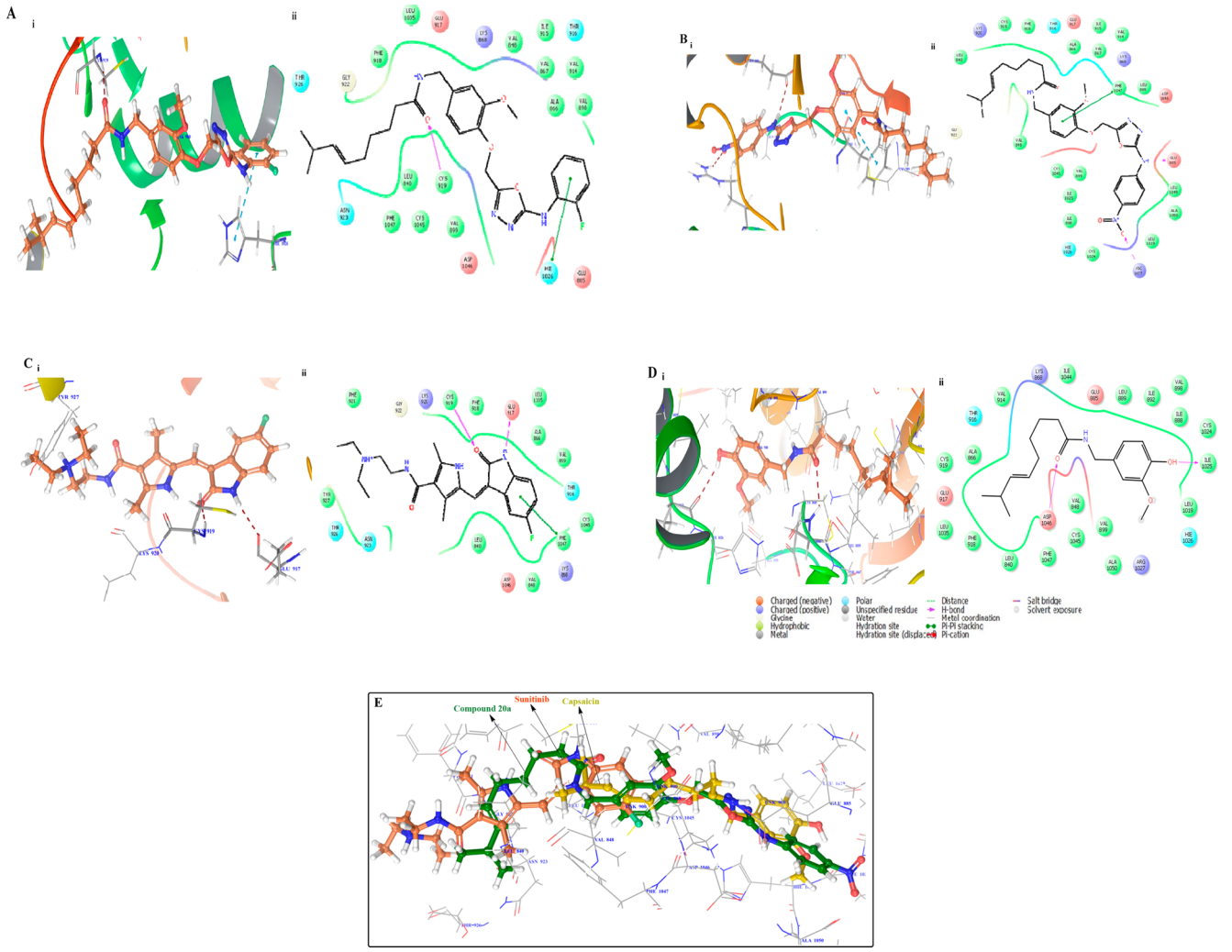

Figure 13. (A) (i) Binding pose of compound **20d** (brown) in the active site of the VEGFR2 kinase receptor with important residues highlighted with gray sticks. (ii) Lig plot of compound **20d**. (B) (i) Binding pose of compound **20a** (brown) in the active site of the VEGFR2 kinase receptor with important residues highlighted with gray sticks. (ii) Lig plot of compound **20d**. (C) (i) Binding pose of standard ligand (Sunitinib) (brown) shown in the active site of the VEGFR2 kinase receptor with important residues highlighted with gray sticks. (D) (i) Binding pose of standard Capsaicin (brown) with important residues enlightened with gray sticks. (ii) Lig plot of compound capsaicin. (E) Superimposition of the docking pose of **20a** (green) with standard sunitinib (orange) and standard capsaicin (yellow) in the active site of the VEGFR2 kinase receptor.

antimigratory effect of compound **20a** acted in a dose dependent manner. Furthermore, Western blot analysis demonstrated a reduction in the expression levels of migration-related protein VEGF in a dose dependent manner (at 1 μM, 2 μM, 5 μM, 10 μM, and 20 μM), while no change in the expression levels of vimentin was found.

Further, **20a** treated NCI-H460 cells were examined for their effect on the expression of some key proliferation markers. The effects of compound **20a** on the expression levels of PCNA, P-53, p-38, p-p38, t-Erk, and p-Erk were determined by Western blotting. The phosphorylation of the MAPK molecule, ERK, and p38 was significantly inhibited at 20 μM concentration of compound **20a** compared to control. However, no change was observed in the expression levels of t-ERK and P53. Also, it was found that compound **20a** reduced the expression levels of cell proliferation marker PCNA in a dose dependent manner (Figure 11). Hence compound **20a** inhibited the key markers related to cell proliferation.

In addition we examined the mRNA expression of VEGFR2 in NCI-H460 cells treated with compound **20a**. VEGFR2 is upregulated in most types of lung cancers, plays an important role in angiogenesis, cell migration, and invasion, and contributes to the aggressive nature of cancer. Our study demonstrated that treatment of compound **20a** significantly reduced the mRNA expression levels of VEGFR2 as revealed by quantitative PCR (Figure 12). This indicates a significant anticancer potential of compound **20a**[26−30] (Figure 12).

All synthesized compounds were docked in the catalytic binding pocket of the VEGFR2 kinase receptor (PDBID: 2QU5) by using schrodinger software to determine their *in silico* binding affinities and their docking score (Table 5).

Herein, the binding pose of the active compounds **20a** and **20d** was reported and compared with the standard cocrystal ligands sunitinib and capsaicin. All compounds were bound in the inactive DFG-Out confirmation (Type II) of the VEGFR2 kinase receptor, in which compound **20d** exhibited the highest docking score of −10.016 (kcal/mol) and demonstrated hydrogen bonding with Cys919 and $\pi-\pi$ stacking with His1026 in the backbone of the VEGFR2 kinase receptor (Figure 13).

https://doi.org/10.1021/acsmedchemlett.1c00304
ACS Med. Chem. Lett. 2021, 12, 1694−1702

Compound **20a** exhibited good cytotoxic activity against the HCT-116, NCI-H60, and SKOV3 cancer cell lines, showed a docking score of −7.528 (kcal/mol), and illustrated hydrogen bonding with Arg1027 and Glu885 and $\pi-\pi$ stacking with the Phe1047 amino acid residue of the VGEFR kinase receptor.

Standard sunitinib having docking score −9.799 (kcal/mol) exhibited hydrogen bonding with Cys 919 and GLU 917 amino acid residues with the $\pi-\pi$ stacking PHE 1047 amino acid residue of the VGEFR kinase receptor, whereas the reference compound capsaicin showed two hydrogen bonds with Asp 1046 and ILE 1025 amino acid residues in the catalytic binding pocket of the VEGFR2 kinase receptor.

In conclusion, a novel series of semisynthetic analogues of capsaicin was synthesized by using a multistep synthetic strategy, and the compounds were screened for their antiproliferative activity. Among all, compound **20a** showed significant antiproliferative activity against the NCI panel of human cancer cell lines (HOP-62, NCI-H460, HCT-116, OVCAR-4, OVCAR-8, SK-OV-3, 786-0, and CAKI-1) with a % growth range of 0−33.6 at 10 μM while compound **20d** also illustrated excellent antiproliferative activity against OVCAR-4 and 786−0 whereas compound **22a** also demonstrated good antiproliferative activity against all the leukemia cancer cell lines with a growth percentage of 29.16−50.23. Among all these three analogues, crystal violet assay showed that compound **20a** illustrated a cytotoxic profile against HCT-116, NCI-H460, and SKOV3 compared with standard capsaicin.

Compound **20a** was further proceed for mechanistic studies, which demonstrated that compound **20a** reduced the clonogenicity potential for the NCI-H460 cancer cell line and significantly increased the ROS production at 20 μM concentration compared to control. Further on, it caused cell arrest at the S phase and induced apoptosis with suppression of Pro-parp and Pro-caspase 3 proteins in NCI-H460. **20a** also exhibited an antimigration property against NCI-H460 cells and restrained the expression of VEGF in a dose dependent manner. Western blot results showed that compound **20a** inhibited the expression of critical markers associated with promoting hypergrowth of cancer cells. Compound **20a** was further screened for determining the expression level of VEGFR2 at the mRNA level. On treatment with compound **20a**, the VEGFR2 (mRNA) was found to be down regulated. All the synthesized compounds were docked in the catalytic binding pocket of the VEGFR2 kinase receptor which revealed that compound **20a** showed a similar kind of binding pattern as that of sunitinib and exhibited a better docking score than capsaicin.

So, the results of this study avowed that compound **20a** may serve as the lead for the discovery of new capsaicin based anticancer agents.

■ ASSOCIATED CONTENT

Supporting Information

The Supporting Information is available free of charge at https://pubs.acs.org/doi/10.1021/acsmedchemlett.1c00304.

Experimental procedures for synthesis of compounds with their analytical data, assay procedure, and ^{1}H NMR, ^{13}C NMR, and mass spectrometry data (PDF)

■ AUTHOR INFORMATION

Corresponding Authors

Yuba Raj Pokharel − *Faculty of Life Sciences and Biology, South Asian University, New Delhi 110021, India*; Email: yrp@sau.ac.in

Syed Shafi − *Department of Chemistry, School of Chemical and Lifescience, Jamia Hamdard, New Delhi 110062, India*; orcid.org/0000-0001-7657-0630; Email: syedshafi@jamiahamdard.ac.in

Authors

Fatima Naaz − *Department of Chemistry, School of Chemical and Lifescience, Jamia Hamdard, New Delhi 110062, India*

Faiz Ahmad − *Faculty of Life Sciences and Biology, South Asian University, New Delhi 110021, India*

Bilal Ahmad Lone − *Faculty of Life Sciences and Biology, South Asian University, New Delhi 110021, India*

Arif Khan − *Department of Chemistry, School of Chemical and Lifescience, Jamia Hamdard, New Delhi 110062, India*

Kalicharan Sharma − *Department of Pharmaceutical Chemistry, School of Pharmaceutical Education and Research, Jamia Hamdard, New Delhi 110062, India*

IntzarAli − *Department of Medical Microbiology, Hamdard Institute of Medical Studies and Research, Jamia Hamdard, New Delhi 110062, India*

M. ShaharYar − *Department of Pharmaceutical Chemistry, School of Pharmaceutical Education and Research, Jamia Hamdard, New Delhi 110062, India*

Complete contact information is available at: https://pubs.acs.org/10.1021/acsmedchemlett.1c00304

Funding

FN is grateful to ICMR, New Delhi, for providing a Research Associate Fellowship with Grant No. 3/2/2/2019/NCD-III. SS is grateful to DST for awarding a fellowship under -DST SERB-ECR/2017/001067/CS.

Notes

The authors declare no competing financial interest.

■ ACKNOWLEDGMENTS

The authors are eternally grateful to Mohammed Nayel (Project Manager), Developmental Therapeutics Program (DTP), at National Cancer Institute, Bethesda, MD, USA, for measuring the *in vitro* antiproliferative activity against a panel of 60 human cancer cell lines.

■ ABBREVIATIONS

ROS, reactive oxygen species; TRPVs, transient receptor potential vanilloids; EDC·HCl, *N*-ethyl-*N*′-(3-(dimethylamino)propyl)carbodiimidehydrochloride; HOBt, hydroxybenzotriazole; NCI, National Cancer Institute; IC_{50}, half maximal inhibitory concentration; VEGF, vascular endothelial growth factor; SAR, structure activity relationship; SD, standard deviation; VEGFR, vascular endothelial growth factor receptor

■ REFERENCES

(1) Patowary, P.; Pathak, M. P.; Zaman, K.; Raju, P. S.; Chattopadhyay, P. Research progress of capsaicin responses to various pharmacological challenges. *Biomed. Pharmacother.* **2017**, *96*, 2017.

(2) Fattori, V.; Hohmann, M. S.; Rossaneis, A. C.; Pinho-Ribeiro, F. A.; Verri, W. A. Capsaicin: Current Understanding of Its Mechanisms

and Therapy of Pain and Other Pre-Clinical and Clinical Uses. *Molecules* **2016**, *21*, 844.
(3) Ito, K.; Nakazato, T.; Yamato, K.; Miyakawa, Y.; Yamada, T.; Hozumi, N.; Segawa, K.; Ikeda, Y.; Kizaki, M. Induction of apoptosis in leukemic cells by homovanillic acid derivative, capsaicin, through oxidative stress: implication of phosphorylation of p53 at Ser-15 residue by reactive oxygen species. *Cancer Res.* **2004**, *64*, 1071.
(4) Gil, Y. G.; Kang, M. K. Capsaicin induces apoptosis and terminal differentiation in human glioma A172 cells. *Life Sci.* **2008**, *82*, 997.
(5) Hail, N.; Lotan, R. Examining the role of mitochondrial respiration in vanilloid-induced apoptosis. *J. Natl. Cancer Inst.***2002**, *94*, 1281.
(6) Caetano, B. F. R.; Tablas, M. B.; Pereira, N. E. F.; de Moura, N. A.; Carvalho, R. F.; Rodrigues, M. A. M.; Barbisan, L. F. Capsaicin reduces genotoxicity, colonic cell proliferation and preneoplastic lesions induced by 1,2-dimethylhydrazine in rats. *Toxicol. Appl. Pharmacol.* **2018**, *338*, 93.
(7) Friedman, J. R.; Perry, H. E.; Brown, K. C.; Gao, Y.; Lin, J.; Stevenson, C. D.; Hurley, J. D.; Nolan, N. A.; Akers, A. T.; Chen, Y. C.; Denning, K. L.; Brown, L. G.; Dasgupta, P. Capsaicin synergizes with camptothecin to induce increased apoptosis in human small cell lung cancers via the calpain pathway. *Biochem. Pharmacol.* **2017**, *129*, 54.
(8) Thoennissen, N. H.; Lu, J. O. K. D.; Iwanski, G. B.; La, D. T.; Abbassi, S.; Leiter, A.; Karlan, R. M.; Koeffler, H. P. Capsaicin causes cell-cycle arrest and apoptosis in ER-positive and -negative breast cancer cells by modulating the EGFR/HER-2 pathway. *Oncogene* **2010**, *29*, 285.
(9) Malagarie-Cazenave, S.; Olea-Herrero, N.; Vara, D.; Morell, C.; Diaz-Laviada, I. The vanilloid capsaicin induces IL-6 secretion in prostate PC-3 cancer cells. *Cytokine* **2011**, *54*, 330.
(10) Ip, S. W.; Lan, S. H.; Lu, H. F.; Huang, A. C.; Yang, J. S.; Lin, J. P.; Huang, H. Y.; Lien, J. C.; Ho, C. C.; Chiu, C. F.; Wood, W.; Chung, J. G. Capsaicin mediates apoptosis in human nasopharyngeal carcinoma NPC-TW 039 cells through mitochondrial depolarization and endoplasmic reticulum stress. *Hum. Exp. Toxicol.* **2012**, *31*, 539.
(11) Wu, C. C.; Lin, J. P.; Yang, J. S.; Chou, S. T.; Chen, S. C.; Lin, Y. T.; Lin, H. L.; Chung, J. G. Capsaicin induced cell cycle arrest and apoptosis in human esophagus epidermoid carcinoma CE 81T/VGH cells through the elevation of intracellular reactive oxygen species and Ca2+ productions and caspase-3 activation. *Mutat. Res., Fundam. Mol. Mech. Mutagen.* **2006**, *601*, 71.
(12) Kim, J. D.; Kim, J. M.; Pyo, J. O.; Kim, S. Y.; Kim, B. S.; Yu, R.; Han, I. S. Capsaicin can alter the expression of tumor forming-related genes which might be followed by induction of apoptosis of a Korean stomach cancer cell line, SNU-1. *Cancer Lett.* **1997**, *120*, 235.
(13) Skrzypski, M.; Sassek, M.; Abdelmessih, S.; Mergler, S.; Grotzinger, C.; Metzke, D.; Wojciechowicz, T.; Nowak, K. W.; Strowski, M. Z. Capsaicin induces cytotoxicity in pancreatic neuroendocrine tumor cells via mitochondrial action. *Cell. Signalling* **2014**, *26*, 41.
(14) Huang, S. P.; Chen, J. C.; Wu, C. C.; Chen, C. T.; Tang, N. Y.; Ho, Y. T.; Lo, C.; Lin, J. P.; Chung, J. G.; Lin, J. G. Capsaicin-induced apoptosis in human hepatoma HepG2 cells. *Anticancer Res.* **2009**, *29*, 165.
(15) Clark, R.; Lee, S. H. Anticancer Properties of Capsaicin Against Human Cancer. *Anticancer research* **2016**, *36*, 837.
(16) Huang, X. F.; Xue, J. Y.; Jiang, A. Q.; Zhu, H. L. Capsaicin and its analogues: structure-activity relationship study. *Curr. Med. Chem.* **2013**, *20*, 2661.
(17) Rollyson, W. D.; Stover, C. A.; Brown, K. C.; Perry, H. E.; Stevenson, C. D.; McNees, C. A.; Ball, J. G.; Valentovic, M. A.; Dasgupta, P. Bioavailability of capsaicin and its implications for drug delivery. *J. Controlled Release* **2014**, *196*, 96.
(18) Reyes-Escogido Mde, L.; Gonzalez-Mondragon, E. G.; Vazquez-Tzompantzi, E. Chemical and pharmacological aspects of capsaicin. *Molecules* **2011**, *16*, 1253.
(19) Gerber, S.; Frueh, B. E.; Tappeiner, C. Conjunctival proliferation after a mild pepper spray injury in a young child. *Cornea* **2011**, *30*, 1042.
(20) Kamaruddin, M. F.; Hossain, M. Z.; Mohamed Alabsi, A.; Mohd Bakri, M. The Antiproliferative and Apoptotic Effects of Capsaicin on an Oral Squamous Cancer Cell Line of Asian Origin, ORL-48. *Medicina (Kaunas)* **2019**, *55*, 322.
(21) Gamal El-Din, M. M.; El-Gamal, M. I.; Abdel-Maksoud, M. S.; Yoo, K. H.; Oh, C. H. Synthesis and broad-spectrum antiproliferative activity of diarylamides and diarylureas possessing 1,3,4-oxadiazole derivatives. *Bioorg. Med. Chem. Lett.* **2015**, *25*, 1692.
(22) Caneschi, W.; Enes, K. B.; Carvalho de Mendonca, C.; de Souza Fernandes, F.; Miguel, F. B.; da Silva Martins, J.; Le Hyaric, M.; Pinho, R. R.; Duarte, L. M.; Leal de Oliveira, M. A.; Dos Santos, H. F.; Paz Lopes, M. T.; Dittz, D.; Silva, H.; Costa Couri, M. R. Synthesis and anticancer evaluation of new lipophilic 1,2,4 and 1,3,4-oxadiazoles. *Eur. J. Med. Chem.* **2019**, *165*, 18.
(23) Valente, S.; Trisciuoglio, D.; De Luca, T.; Nebbioso, A.; Labella, D.; Lenoci, A.; Bigogno, C.; Dondio, G.; Miceli, M.; Brosch, G.; Del Bufalo, D.; Altucci, L.; Mai, A. 1,3,4-Oxadiazole-Containing Histone Deacetylase Inhibitors: Anticancer Activities in Cancer Cells. *J. Med. Chem.* **2014**, *57*, 6259.
(24) Ragab, F. A. F.; Abou-Seri, S. M.; Abdel-Aziz, S. A.; Alfayomy, A. M.; Aboelmagd, M. Design, synthesis and anticancer activity of new monastrol analogues bearing 1,3,4-oxadiazole moiety. *Eur. J. Med. Chem.* **2017**, *138*, 140.
(25) Fathi, M. A. A.; Abd El-Hafeez, A. A.; Abdelhamid, D.; Abbas, S. H.; Montano, M. M.; Abdel-Aziz, M. 1,3,4-oxadiazole/chalcone hybrids: Design, synthesis, and inhibition of leukemia cell growth and EGFR, Src, IL-6 and STAT3 activities. *Bioorg. Chem.* **2019**, *84*, 150.
(26) Wang, N.; Chen, H.; Teng, Y.; Ding, X.; Wu, H.; Jin, X. Artesunate inhibits proliferation and invasion of mouse hemangioendothelioma cells in vitro and of tumor growth in vivo. *Oncol. Lett.* **2017**, *14*, 6170.
(27) Shibuya, M. Vascular endothelial growth factor (VEGF)-Receptor2: its biological functions, major signaling pathway, and specific ligand VEGF-E. *Endothelium* **2006**, *13*, 63.
(28) Zhan, P.; Ji, Y.-N.; Yu, L.-K. VEGF is associated with the poor survival of patients with prostate cancer: a meta-analysis. *Transl. Androl. Urol.* **2013**, *2*, 99.
(29) Su, F.; Liu, B.; Chen, M.; Xiao, J.; Li, X.; Lv, X.; Ma, J.; You, K.; Zhang, J.; Zhang, Y. Association between VEGF-A, C and D expression and lymph node involvement in breast cancer: a meta-analysis. *Int. J. Biol. Markers* **2016**, *31*, 235.
(30) Mazeda, I.; Martins, S. F.; Garcia, E. A.; Rodrigues, M.; Longatto, A. VEGF Expression in Colorectal Cancer Metastatic Lymph Nodes: Clinicopathological Correlation and Prognostic Significance. *Gastrointest. Disord.* **2020**, *2*, 267.

https://doi.org/10.1021/acsmedchemlett.1c00304
ACS Med. Chem. Lett. 2021, 12, 1694−1702